Bethe-Salpeter study of vector meson masses and decay constants

Pieter Maris and Peter C. Tandy
Center for Nuclear Research, Department of Physics, Kent State University, Kent, Ohio 44242
(Received 27 May 1999; published 21 October 1999)

The masses and decay constants of the light vector mesons ρ/ω, ϕ, and $K^\star$ are studied within a ladder-rainbow truncation of the coupled Dyson-Schwinger and Bethe-Salpeter equations of QCD with a model two-point gluon function. The approach is consistent with quark and gluon confinement, reproduces the correct one-loop renormalization group behavior of QCD, generates dynamical chiral symmetry breaking, and preserves the relevant Ward identities. The one phenomenological parameter and two current quark masses are fixed by requiring that the calculated f_π, m_π, and m_K are correct. The resulting f_K is within 3% of the experimental value. For the vector mesons, all eight transverse covariants are included and the dominant ones are identified; the complete angle dependence of the amplitudes is also retained. The calculated values for the masses m_ρ, m_ϕ, and $m_{K^\star}$ are within 5%, while the decay constants f_ρ, f_ϕ, and $f_{K^\star}$ for electromagnetic and leptonic decays are within 10% of the experimental values. [S0556-2813(99)04511-2]

PACS number(s): 14.40.Cs, 24.85.+p, 11.10.St, 12.38.Lg

I. INTRODUCTION

A realistic description of vector mesons at the quark-gluon level is an important element in advancing our understanding of hadron dynamics and reaction processes at scales where QCD degrees of freedom are relevant. They are easily produced as decay products in electroexcitation of baryon resonances and also as precursors to dilepton events in relativistic heavy-ion collisions. Flavorless vector mesons couple directly to the photon and play an important role in the phenomenology of electromagnetic coupling to hadrons. This is exemplified by the general phenomenological success of the vector meson dominance model which assumes that the electromagnetic current is saturated by the vector mesons. The ground state vector mesons, being spin modes, sample the $q\bar{q}$ bound state dynamics in a way that is complementary to that of the ground state pseudoscalar (PS) mesons. They also explore quark and gluon confinement since the vector masses are greater than the sum of typical constituent quark masses. Mesonic strong decays such as $\rho\to\pi\pi$ and $\phi\to KK$, radiative decays such as $\rho\to\pi\gamma$ and $K^\star\to K\gamma$, and electromagnetic decays such as $\rho^0\to e^+e^-$ and $\phi\to e^+e^-$ can probe aspects of the underlying quark-gluon dynamics that are complementary to what is learned from PS mesons.

The PS mesons, especially the pion and kaon, have for a long time been a major focus of attempts to understand the internal structure of hadrons from nonperturbative QCD. Chiral symmetry provides an assistance in the PS case that is not available to other mesons such as the vectors we discuss in this paper. In the chiral limit of massless QCD, the dynamical breaking of chiral symmetry generates masses for the light quarks that are consistent with the empirical constituent masses deduced from the hadronic spectrum. The lowest PS mesons, which would be massless in this limit as dictated by the Goldstone theorem, acquire a mass through the explicit breaking of chiral symmetry induced by the current quark masses. This phenomenon dominates the systematics of the ground state PS octet and provides chiral Ward identities that relate dynamical quantities in a way that simplifies somewhat the task of modeling low energy QCD. For example, the axial Ward identity dictates that the chiral limit Bethe-Salpeter (BS) amplitude for a pseudoscalar $q\bar{q}$ bound state in the dominant γ_5 channel is given by $B_0(p^2)/f_P$ where B_0 is the scalar part of the chiral quark self-energy, and f_P is the meson weak decay constant. Consideration of the symmetry breaking effect of current masses within the PS bound state dynamics leads to an exact formula for m_P the PS meson mass [1]. One corollary is the Gell-Mann–Oakes–Renner relation at small current quark masses where $m_P\propto\sqrt{m_q}$; a second corollary is the behavior $m_P\propto m_Q$ for heavy quark PS mesons [2]. With these aids, an efficient and qualitatively useful phenomenology for observables and other quantities associated with the pion and kaon can be produced without explicit solution of the bound state Bethe-Salpeter equation (BSE). The only dynamical input required is the dressed quark propagator as defined by the quark Dyson-Schwinger equation (DSE).

The study of hadronic processes is often facilitated by parametrizing DSE quark propagator solutions into analytic forms with a few parameters readjusted to accommodate chiral observables [3]. With such an approach, $m_{\pi/K}$ and $f_{\pi/K}$, the charge radii $r_{\pi/K}$ and form factors $F_{\pi/K}(Q^2)$, and the π-π scattering lengths have been well described [3]. This approach has also been successful in studies of coupling constants and form factors for processes such as $\pi^0\to\gamma\gamma$ [4] and $\gamma\pi\to\pi\pi$ [5]. The incorporation of vector mesons has been hindered by the lack of a symmetry-based means of obtaining approximate dynamical insight without direct solution of the vector BSE. There is a conserved current and a corresponding vector Ward-Takahashi identity linking the longitudinal vector vertex with the quark propagator. However, this Ward identity does not constrain the transverse vector meson BS amplitude and therefore purely phenomenological vector BS amplitudes have often been used to study processes involving vector mesons in this framework. Successful applications of this type include the decays $\rho\to\pi\pi$ and $\rho\to\pi\gamma$ [6,7] and diffractive electroproduction of vector mesons [8]. Uncertainties concerning contributions to hadronic observables from the neglected covariants in the PS meson BS amplitudes beyond the canonical γ_5 were not

addressed until recently [9,10]. Several studies [9,11] also incorporated some aspects of vector BSE dynamics and were able to make a crude assessment of the role of subdominant covariants of the rho [12] in $\rho\to\pi\pi$ and $\rho\to\pi\gamma$ but at the expense of using a separable *Ansatz* [9] for the BSE kernel. A recent study of heavy meson decays also employs phenomenological BS amplitudes for vector mesons [2].

The persistent outcome of the above studies is that soft observables associated with the pion and kaon are consistently and naturally described in terms of the momentum dependent quark self-energy from realistic solutions [13] of the quark DSE. Important to the success of this approach are the features of quark confinement and dynamical chiral symmetry breaking that are implemented through a strong enhancement in the infrared behavior of the effective quark-quark interaction (or effective gluon two-point function [14]) in rainbow approximation. In the light pseudoscalar sector, the most comprehensive and quantitatively reliable study to date [10] involves direct solution of the bound state BSE in conjunction with quark DSE solutions for propagators. That work represents the development of an appropriate phenomenological representation for the infrared structure of the gluon two-point function in conjunction with a bare quark-gluon vertex so that the DSE solution for the quark propagator exhibits dynamical chiral symmetry breaking as well as confinement [15] and, through the BSE, produces a good description soft pion and kaon observables. One of the aims of Ref. [10] was an exposition of the detailed numerical consequences of the constraint provided by the axial vector Ward-Takahashi identity (AV-WTI) upon PS meson dynamics. This constraint is formally assured by the coordinated rainbow-ladder truncation of the DSE-BSE complex of DSEs. The inclusion of all possible covariants for the BS amplitude was found necessary to numerically preserve the constraint and to obtain quantitatively accurate observables. Of general importance are two other advances represented by Ref. [10]. First, since the ultraviolet structure of the model is equipped with the one-loop renormalization group properties from perturbative QCD, it is a realistic and covariant hadron model that can be unambiguously evolved in scale. Secondly, it is produced by well-defined truncations of the QCD equations of motion (DSEs), and thus can be systematically improved by including higher-order corrections to the quark-antiquark scattering kernel.

The extension of the DSE approach to vector mesons is explored here. Solution of the vector BSE is more difficult than in the PS case because of the significantly larger number of covariants that must be investigated and also because the higher masses produce a larger domain of the quark complex p^2 plane that must be sampled. This latter issue was avoided in a previous work [16] that made an extensive study of the meson spectrum from the ladder-rainbow truncation of the DSE-BSE system. In that approach, a derivative expansion of the quark self-energy was used to infer the behavior away from the real axis and some attempt was made to estimate the resulting error. The implications for quark confinement in that approach are unclear. One of our aims here is to generate vector meson BS amplitudes without compromising the analytic structure in a way that may impair the subsequent explorations of meson decays and form factors. These amplitudes can then be used to calibrate and guide approximate representations that simplify the study of hadronic interactions.

In this paper we calculate the ground state vector mesons ρ/ω, $K^\star$, and ϕ in the DSE-BSE approach, using the ladder-rainbow truncation. The effective quark-quark interaction is fixed by pion and kaon properties and we investigate the quality of generated vector meson masses and decay constants. In Sec. II we outline the framework of the DSE approach we employ along with the truncation and the *Ansatz* we use to specify the kernel (or effective gluon two-point function) for both the quark DSE and the bound state BSE. Our investigations are conducted with a variation of the kernel *Ansatz* that was developed in Ref. [10] for the pion and kaon. To facilitate the analysis and solution of the vector BSE, we have employed a convenient set of eight Dirac covariants that satisfy both the CPT constraints and a trace-orthogonality property. These are presented and discussed in Sec. III. Also in that section we outline the technique of expansion of the amplitudes in terms of Chebyshev polynomials that is sometimes used to resolve the angle dependence and reduce the BSE to a set of one-dimensional equations. In Sec. IV the meson decay constants treated here are defined. Results are presented and discussed in Sec. V, and a summary and conclusion follows in Sec. VI. Some technical details are collected in an Appendix.

II. DYSON-SCHWINGER EQUATIONS

In a Euclidean space formulation, with $\{\gamma_\mu,\gamma_\nu\}=2\delta_{\mu\nu}$, $\gamma_\mu^\dagger=\gamma_\mu$ and $a\cdot b=\sum_{i=1}^4 a_i b_i$, the DSE for the renormalized dressed-quark propagator is

$$S(p)^{-1}=Z_2 i\gamma\cdot p+Z_4 m(\mu)+Z_1\int_q^\Lambda g^2 D_{\mu\nu}(p-q)\frac{\lambda^a}{2}\gamma_\mu S(q)\Gamma_\nu^a(q,p), \quad (1)$$

where $D_{\mu\nu}(k)$ is the renormalized dressed-gluon propagator, $\Gamma_\nu^a(q;p)$ is the renormalized dressed-quark-gluon vertex, and $\int_q^\Lambda\equiv\int^\Lambda d^4q/(2\pi)^4$ represents mnemonically a translationally invariant regularization of the integral, with Λ the regularization mass scale. The final stage of any calculation is to remove the regularization by taking the limit $\Lambda\to\infty$. The solution of Eq. (1) has the general form

$$S(p)^{-1}=i\gamma\cdot pA(p^2,\mu^2)+B(p^2,\mu^2), \quad (2)$$

and the renormalization condition is

$$S(p)^{-1}|_{p^2=\mu^2}=i\gamma\cdot p+m(\mu), \quad (3)$$

at a sufficiently large spacelike μ^2, with $m(\mu)$ the renormalized quark mass at the scale μ. The renormalization constants for the quark-gluon-vertex, the quark wave function, and the mass, namely, $Z_1(\mu^2,\Lambda^2)$, $Z_2(\mu^2,\Lambda^2)$, and $Z_4(\mu^2,\Lambda^2)$, respectively, depend on the renormalization point and the regularization mass scale. In Eq. (1), S, Γ_μ^a,

and $m(\mu)$ depend on the quark flavor, although we have not indicated this explicitly. However, in our analysis we assume, and employ, a flavor independent renormalization scheme and hence all the renormalization constants are flavor-independent.

A. Meson Bethe-Salpeter equation

The renormalized, homogeneous BSE for a bound state of a quark of flavor a and an antiquark of flavor b having total momentum P is given by

$$\Gamma_M^{ab}(p;P)=\int^{\Lambda}\frac{d^4q}{(2\pi)^4}K(p,q;P) \times S^a(q+\eta P)\Gamma_M^{ab}(q;P)S^b(q-\bar{\eta}P), \quad (4)$$

where $\eta+\bar{\eta}=1$ describes momentum sharing, $\Gamma_M^{ab}(p;P)$ is the BS amplitude, and M specifies the meson type: pseudoscalar, vector, axial-vector, or scalar. In this paper we consider the pseudoscalar and vector amplitudes only. The kernel K operates in the direct product space of color and Dirac spin for the quark and antiquark and is the renormalized, amputated $\bar{q}q$ scattering kernel that is irreducible with respect to a pair of $\bar{q}q$ lines. It is often convenient to express Eq. (4) in the abbreviated form

$$[\Gamma_M^{ab}(p;P)]_{tu}=\int_q^{\Lambda}K_{tu}^{rs}(p,q;P)[\chi_M^{ab}(q;P)]_{sr}, \quad (5)$$

where $\chi_M^{ab}(q;P)\equiv S^a(q_+)\Gamma_M^{ab}(q;P)S^b(q_-)$ is the BS wave function, $q_+\equiv q+\eta P$, $q_-\equiv q-\bar{\eta}P$, and the labels $r,\ldots,u$ represent color- and Dirac-matrix indices. This equation defines an eigenvalue problem with physical solutions at the mass-shell points $P^2=-m^2$ with m being the bound state mass.

The canonical normalization condition of the solution of the homogeneous BSE is

$$2P_\mu=\frac{\partial}{\partial P_\mu}\Bigg\{\int_q^{\Lambda}\mathrm{Tr}_{CD}[\bar{\Gamma}_M^{ba}(q;-K)S^a(q+\eta P) \times\Gamma_M^{ab}(q;K)S^b(q-\bar{\eta}P)] + \int_q^{\Lambda}\int_k^{\Lambda}[\bar{\chi}_M^{ba}(k;-K)]_{ut}K_{tu}^{rs}(k,q;P) \times[\chi_M^{ab}(q;K)]_{sr}\Bigg\}\Bigg|_{P^2=K^2=-m^2}, \quad (6)$$

where $\bar{\Gamma}_M(k,-P)^{\mathrm{t}}=C^{-1}\Gamma_M(-k,-P)C$, in which $C=\gamma_2\gamma_4$ is the charge conjugation matrix, and X^{t} denotes the matrix transpose of X. The trace in the first term is over both color and Dirac indices. If the quark-antiquark scattering kernel K is independent of the total momentum P, as is the case in the ladder truncation we consider here, then the second term vanishes.

B. Ladder-rainbow truncation

We use a ladder truncation for the BSE

$$K_{tu}^{rs}(p,q;P)\to-\mathcal{G}[(p-q)^2]D_{\mu\nu}^{\mathrm{free}}(p-q)\left(\frac{\lambda^a}{2}\gamma_\mu\right)^{ru} \otimes\left(\frac{\lambda^a}{2}\gamma_\nu\right)^{ts}, \quad (7)$$

which is consistent with a rainbow truncation for the quark DSE

$$Z_1\int_q^{\Lambda}g^2D_{\mu\nu}(p-q)\frac{\lambda^a}{2}\gamma_\mu S(q)\Gamma_\nu^a(q,p) \to\int_q^{\Lambda}\mathcal{G}[(p-q)^2]D_{\mu\nu}^{\mathrm{free}}(p-q)\frac{\lambda^a}{2}\gamma_\mu S(q)\frac{\lambda^a}{2}\gamma_\nu. \quad (8)$$

Here $D_{\mu\nu}^{\mathrm{free}}(k)$ is the perturbative gluon propagator in Landau gauge. The model is completely specified once a form is chosen for the ''effective coupling'' $\mathcal{G}(k^2)$.

The consistency of Eqs. (7) and (8) lies in the fact that the axial-vector Ward-Takahashi identity is preserved [1,10]. This ensures that in the chiral limit the ground state PS mesons are massless even though the quark mass functions are strongly enhanced in the infrared. In the physical case of explicit chiral symmetry breaking, it also ensures an exact relation between the PS meson mass and weak decay constant, the current quark masses, and the residue at the PS meson pole in the PS vertex [1,10]. The analysis in Ref. [17] shows that the next-order contributions to the kernel in a quark-gluon skeleton graph expansion, have a significant amount of cancellation between repulsive and attractive corrections for pseudoscalar mesons. Indications are that this is also the case in the vector channel, which strongly supports the use of ladder truncations in these cases.

In choosing a form for $\mathcal{G}(k^2)$ we know that the behavior of the QCD running coupling $\alpha(k^2)$ in the ultraviolet, i.e., for $k^2>2$–$3\ \mathrm{GeV}^2$, is well described by perturbation theory. In principle, constraints on the infrared form of $\mathcal{G}(k^2)$ can be sought from studies of the DSEs satisfied by the dressed gluon propagator $D_{\mu\nu}(k)$ and the dressed gluon-quark vertex $\Gamma_\nu^a(q,p)$. The latter is often represented by an *Ansatz*; there is almost no information available from DSE studies; the gluon propagator has been often studied via its DSE. If the ghost loop and the quark loop in the gluon DSE are unimportant, then the qualitative conclusion from such studies is that the gluon propagator is significantly enhanced in the infrared and well represented by an integrable singularity such as a regularization of $1/k^4$ [14]. Phenomenological studies containing such an enhancement show that dynamical chiral symmetry breaking and quark confinement follow in a straightforward and natural way from the quark DSE with an empirically correct value for the chiral condensate $\langle\bar{q}q\rangle^0$ and an excellent description of pion and kaon properties [10].

Recent gluon DSE studies that include the ghost loop but not the quark loop have suggested a weak infrared strength that vanishes at $k^2=0$ for the transverse component of

$D_{\mu\nu}(k)$ due to a strong infrared enhancement of the ghost propagator [18,19]. In some studies of this type, unphysical particlelike singularities occur in the *Ansatz* for the dressed ghost-gluon and three-gluon vertices [18]. It is apparent that such gluon DSE studies are presently limited by the type of truncation that can be accommodated and the preliminary nature of the *Ansätze* employed for some of the dressed vertices. Several lattice studies of $D_{\mu\nu}(k)$ have been interpreted in terms of an infrared behavior less singular than $1/k^2$ [20]. The phenomenological implications of either type of nonsingular infrared behavior for $D_{\mu\nu}(k)$ have recently been explored within the quark DSE [21]. It was found that dynamical chiral symmetry breaking as represented by a nonzero chiral condensate is either absent or is a small fraction of what is required to explain pion phenomena; the produced quark propagator does not show quark confinement.

To provide a quark DSE-based description of pion and kaon phenomena as a basis for exploring vector meson properties, we utilize a variation of the following *Ansatz* introduced in Ref. [10]:

$$\frac{\mathcal{G}(k^2)}{k^2} = 8\pi^4 D\delta^4(k) + \frac{4\pi^2}{\omega^6} D k^2 e^{-k^2/\omega^2} + 4\pi \frac{\gamma_m \pi}{(1/2)\ln[\tau + (1 + k^2/\Lambda_{\rm QCD}^2)^2]} \mathcal{F}(k^2), \quad (9)$$

with $\mathcal{F}(k^2) = \{1 - \exp(-k^2/[4m_t^2])\}/k^2$, $\tau = e^2 - 1$, and $\gamma_m = 12/(33 - 2N_f)$. This *Ansatz* preserves the one-loop renormalization group behavior of QCD for solutions of the quark DSE. In particular, the correct one-loop QCD anomalous dimension of the quark mass function $M(p^2)$ is preserved in its ultraviolet behavior for both the chiral limit [$m(\mu) = 0$, anomalous dimension $1 - \gamma_m$] and explicit chirally broken case [$m(\mu) \neq 0$, anomalous dimension γ_m]. This asymptotic behavior, a characteristic of QCD, is confirmed by analysis of the numerical solution in the ultraviolet as described in detail in Ref. [10]. The main qualitative feature of Eq. (9) is that the phenomenologically required strong infrared enhancement in the region $0-0.5$ GeV^2 is distributed over an integrable $\delta^4(k)$ singularity [22] and a finite-width approximation to $\delta^4(k)$ normalized so that both terms have the same $\int d^4k$. The last term in Eq. (9) is proportional to $\alpha(k^2)/k^2$ at large spacelike k^2 and has no singularity on the real k^2 axis. The parameters ω and m_t were not varied freely in the study of Ref. [10]; the fixed values $m_t = 0.5$ GeV and $\omega = 0.3$ GeV were chosen mainly to ensure that $\mathcal{G}(k^2) \approx 4\pi\alpha(k^2)$ for $k^2 > 2$ GeV^2. The free parameters were D and the renormalized u/d- and s-quark current masses to obtain a good description of π and K properties.

Solutions of the rainbow DSE for the quark propagator, when investigated, usually reveal a nonanalytic behavior in the complex p^2 plane often in the form of complex conjugate branch points [23,24] that are modified or even eliminated when the gluon-quark vertex is dressed [25]. Subsequent use of the propagator solutions in the BSE for the bound state meson should be accompanied by a determination that such nonanalytic points (that are likely artifacts of the truncation) lie outside the complex domain of integration that naturally arises in the search for a solution of the BSE in Euclidean metric. The mass of the meson determines the extent of the required departures from the quark real p^2 axis and the pion and kaon solutions from the *Ansatz* of Eq. (9) are free of such problems. However, with the parameters of Ref. [10], we have found this not to be the case for the more massive vector solutions. For the present study of vector mesons, we eliminate the δ-function term from Eq. (9) and increase the strength of the second (finite-width) term so that it alone implements the infrared enhancement. The quark confinement and dynamical chiral symmetry breaking properties are preserved because the essential feature, the integrated strength in the infrared domain, remains. The removal of the δ-function term allows parameters to be easily found to produce quark DSE solutions that are smooth functions in the entire integration domain required for the vector mesons considered here as well as for the pion and kaon; the quality of the pseudoscalar results is preserved.

We therefore employ the *Ansatz*

$$\frac{\mathcal{G}(k^2)}{k^2} = \frac{4\pi^2}{\omega^6} D k^2 e^{-k^2/\omega^2} + 4\pi \frac{\gamma_m \pi}{(1/2)\ln[\tau + (1 + k^2/\Lambda_{\rm QCD}^2)^2]} \mathcal{F}(k^2). \quad (10)$$

As in the earlier pion and kaon studies, we use $m_t = 0.5$ GeV, $\tau = e^2 - 1$, $N_f = 4$, $\Lambda_{\rm QCD}^{N_f=4} = 0.234$ GeV, and a renormalization point $\mu = 19$ GeV, which is sufficiently perturbative to allow the one-loop asymptotic behavior of the quark propagator to be used as a check. We consider three parameter sets characterized by three different values of ω. For each parameter set, D is treated as a phenomenological parameter, which was fitted, along with the renormalized current quark masses, to obtain a good description of $m_{\pi/K}$ and f_π. Subsequently, the vector meson sector was studied without parameter adjustment. For comparison we also report, for the *Ansatz* of Ref. [10], vector meson masses estimated by an extrapolation of the BSE eigenvalue to the mass-shell point.

III. VECTOR MESON BETHE-SALPETER AMPLITUDES

The general form of a vector vertex $\Gamma_\mu(q;P)$ can be expressed as a decomposition into twelve independent Lorentz covariants, made from the three vectors γ_μ, the relative momentum q_μ, and the meson total momentum P_μ, each multiplied by one of the four independent matrices (1), $\gamma\cdot q$, $\gamma\cdot P$, and $\sigma_{\mu\nu}q_\mu P_\nu$. Since a vector meson BS amplitude is transverse the number of allowed covariants reduces to 8, so that the general decomposition of the vector BS amplitude is

$$\Gamma_\mu^V(q;P) = \sum_{i=1}^{8} T_\mu^i(q;P) F_i(q^2, q\cdot P; P^2), \quad (11)$$

with the invariant amplitudes $F_i(q^2, q\cdot P; P^2)$ being Lorentz scalar functions. The choice for the covariants $T_\mu^i(q;P)$ to be

used as a basis is constrained by the required properties under Lorentz and parity transformations, but is not unique. The BSE equation (4) must be projected onto the covariant basis to produce a coupled set of eight linear equations for the invariant amplitudes F_i to be cast in matrix form. This requires a procedure to project out a single amplitude from the general form (11). It is therefore helpful if the chosen covariants satisfy a Dirac-trace orthonormality property.

We have chosen the following set of dimensionless orthogonal covariants:

$$T^1_\mu(q;P)=\gamma^T_\mu, \tag{12}$$

$$T^2_\mu(q;P)=\frac{6}{q^2\sqrt{5}}[q^T_\mu(\gamma^T\cdot q)-\tfrac{1}{3}\gamma^T_\mu(q^T)^2], \tag{13}$$

$$T^3_\mu(q;P)=\frac{2}{qP}[q^T_\mu(\gamma\cdot P)], \tag{14}$$

$$T^4_\mu(q;P)=\frac{i\sqrt{2}}{qP}[\gamma^T_\mu(\gamma\cdot P)(\gamma^T\cdot q)+q^T_\mu(\gamma\cdot P)], \tag{15}$$

$$T^5_\mu(q;P)=\frac{2}{q}q^T_\mu, \tag{16}$$

$$T^6_\mu(q;P)=\frac{i}{q\sqrt{2}}[\gamma^T_\mu(\gamma^T\cdot q)-(\gamma^T\cdot q)\gamma^T_\mu], \tag{17}$$

$$T^7_\mu(q;P)=\frac{i\sqrt{3}}{P\sqrt{5}}(1-\cos^2\theta)[\gamma^T_\mu(\gamma\cdot P)-(\gamma\cdot P)\gamma^T_\mu]$$
$$-\frac{1}{\sqrt{2}}T^8_\mu(q;P), \tag{18}$$

$$T^8_\mu(q;P)=\frac{i2\sqrt{6}}{q^2P\sqrt{5}}q^T_\mu(\gamma^T\cdot q)(\gamma\cdot P), \tag{19}$$

where V^T is the component of V transverse to P

$$V^T_\mu=V_\mu-\frac{P_\mu(P\cdot V)}{P^2}, \tag{20}$$

and $q\cdot P=qP\cos\theta$. Note that at the mass-shell $P=im$. The orthonormality property satisfied by these covariants is

$$\tfrac{1}{12}\mathrm{Tr}_D[T^i_\mu(q;P)T^j_\mu(q;P)]=f_i(\cos\theta)\delta_{ij}, \tag{21}$$

where the functions $f_i(z)$ are given by $f_1(z)=1$, $f_i(z)=\frac{4}{3}(1-z^2)$ for $i=3,4,5,6$ and $f_i(z)=\frac{8}{5}(1-z^2)^2$ for $i=2,7,8$. For later use we also note the relation

$$\int_0^\pi d\theta\sin^2\theta\ f_i(\cos\theta)=\frac{\pi}{2}. \tag{22}$$

The covariants are dimensionless and independent of the magnitudes q and P. These properties are helpful in allowing the relative magnitude of the amplitudes F_i to be a qualitative measure of the dynamical importance of the various covariants. A more quantitative measure can depend on the particular observable being studied; amplitudes that are unimportant at low momenta can become dominant when high momentum behavior of the bound state solution is being probed.

For unflavored mesons that are eigenstates of C (charge conjugation), such as the ρ, ω, and ϕ, there is an additional constraint on the BS amplitude[1] to obtain a specified C-parity. Of the eight covariants given in Eqs. (12)–(19), T^3 and T^6 are even under C, the others are odd under C. The only remaining quantity that can produce a desired uniform C-parity is $q\cdot P$ which is odd under C. Thus a $C=-1$ solution (such as the ρ and ϕ) will have amplitudes F_3 and F_6 that are odd in $q\cdot P$ while the remaining amplitudes are even in $q\cdot P$. For the flavored vector meson $K^\star$, which is not an eigenstate of C, each amplitude will contain both even and odd terms in $q\cdot P$. Since the ladder truncation of the BSE is invariant under charge conjugation if equal momentum sharing ($\eta=0.5$) is used, the observation of the above odd-even behavior in $q\cdot P$ of F_i can be used as a test of numerical accuracy. Alternatively, the amplitudes F_i can be expanded in terms of a basis of functions that are appropriately odd or even in $\cos\theta$ to save significantly on computer time and memory. Because the mass-shell condition makes the magnitude P imaginary, it is not difficult to verify that with definite C parity, each amplitude associated with our chosen basis of covariants is either purely real or purely imaginary. The amplitudes F_i for the $K^\star$ solution are in general complex due to the dependence upon all powers of $q\cdot P$.

After using representation (11) for the solution in terms of the covariant basis, followed by projection using the Dirac-trace orthonormality property (21), the homogeneous BSE equation (4) for a meson with flavored constituents $a\bar{b}$ reduces to a set of coupled integral equations for the eight functions $F^{ab}_i(q^2,q\cdot P;P^2)$ in the form

$$F^{ab}_i(p^2,p\cdot P;P^2)f_i(z)$$
$$=-\tfrac{4}{3}\int^\Lambda\frac{d^4q}{(2\pi)^4}\mathcal{G}[(p-q)^2]D^{\mathrm{free}}_{\mu\nu}(p-q)F^{ab}_j(q^2,qP;P^2)$$
$$\times\tfrac{1}{12}\mathrm{Tr}_D[T^i_\rho(p;P)\gamma_\mu S^a(q+\eta P)T^j_\rho(q;P)S^b(q-\overline{\eta}P)\gamma_\nu]. \tag{23}$$

The above system of equations was solved by two complementary methods. The first method was a direct treatment as an integral eigenvalue equation $\lambda(P^2)\mathsf{F}=\mathsf{K}(P^2)\mathsf{F}$ for a set of functions F of two variables p^2 and $z=\cos\theta$. An iterative method is used to determine the smallest m satisfying

[1]We do not discriminate between up and down quarks, and do not take into account electromagnetic corrections; therefore the BS amplitudes for $\rho^\pm$ are equal to those for ρ^0. Furthermore, the ladder truncation cannot discriminate between isovector and isoscalar mesons; therefore the ρ and the ω are degenerate in this truncation.

$\lambda(-m^2)=1$. Both variables were discretized via Gaussian quadrature and the summations for the double integration were carried out at each iteration. This has a high demand on computer memory.

In the second method, the angle dependence of the amplitudes is expanded in the form

$$F_i(q^2,qP;P^2)=\sum_{j=0}^{\infty} {}^jF_i(q^2;P^2)U_j(\cos\theta), \tag{24}$$

where the $U_j(z)$ are Chebyshev polynomials of the second kind. This allows the angle integrations in Eq. (23) to be carried out to produce an integral equation in one variable but for a larger set of functions ${}^jF_i(q^2;P^2)$. For $C=-1$ eigenstates such as ρ and ϕ, amplitudes F_3 and F_6 will require only odd order Chebyshev terms while the other amplitudes will require only even terms. In practice, the number of Chebyshev terms required is quite low (one or two terms) so that the memory requirements are effectively reduced in this second method. The solutions from the direct two-variable approach can be projected onto the Chebyshev basis as a check on the second method and also as a means of presentation.

The specific normalization condition for the vector meson solutions of the ladder BSE follows from Eq. (6) and is

$$2P_\mu=\frac{\partial}{\partial P_\mu}\frac{N_c}{3}\int_q^\Lambda \mathrm{Tr}_D[\overline{\Gamma}_\nu^{ba}(q;-K)S^a(q+\eta P) \times\Gamma_\nu^{ab}(q;K)S^b(q-\overline{\eta}P)]|_{P^2=K^2=-m^2}, \tag{25}$$

where the factor 1/3 appears because the three transverse directions are summed.

IV. ELECTROWEAK DECAY

Here we summarize the definition of, and our convention for, the vector meson leptonic and electromagnetic decay constants and their explicit relationship to the BS amplitudes. The electromagnetic decay mediated by a photon (e.g., ρ^0, ω, ϕ), and the leptonic decay mediated by a W boson (e.g., $\rho^\pm$, $K^{\star\pm}$), are described by the vector decay constant defined by [26]

$$f_V m_V \epsilon_\mu^{(\lambda)}(P)=\langle 0|\overline{q}^b\gamma_\mu q^a|V^{ab}(P,\lambda)\rangle, \tag{26}$$

where $\epsilon_\mu^{(\lambda)}$ is the polarization vector of the vector meson satisfying $\epsilon^{(\lambda)}\cdot P=0$ and normalized such that $\epsilon_\mu^{(\lambda)*}\epsilon_\mu^{(\lambda)}=3$. This is completely analogous to the definition

$$f_P P_\mu=\langle 0|\overline{q}^b\gamma_\mu\gamma_5 q^a|P^{ab}(P)\rangle \tag{27}$$

for the pseudoscalar decay constant that corresponds to $f_\pi=131$ MeV under the normalization convention of Eq. (6). The vector decay constant from Eq. (26) can be expressed as the loop integral

$$f_V m_V=\frac{Z_2 N_c}{3}\int^\Lambda\frac{d^4q}{(2\pi)^4} \times\mathrm{Tr}_D[\gamma_\mu S^a(q+\eta P)\Gamma_\mu^{ab}(q;P)S^b(q-\overline{\eta}P)], \tag{28}$$

which is exact if the dressed quark propagators and the meson BS amplitude are exact [2]. In the next section we use Eq. (28) to calculate the decay constants f_ρ, f_ϕ, and $f_{K^\star}$.

The coupling of the ρ^0

$$|\rho^0\rangle=\frac{1}{\sqrt{2}}(|u\overline{u}\rangle-|d\overline{d}\rangle) \tag{29}$$

to the photon is conventionally expressed via a dimensionless coupling constant g_ρ in the form

$$\frac{m_\rho^2}{g_\rho}\epsilon_\mu^{(\lambda)}(P)=\langle 0|\overline{\mathcal{Q}}\hat{Q}\gamma_\mu\mathcal{Q}|\rho^0(P,\lambda)\rangle, \tag{30}$$

where the flavor multiplet of quark field spinors is $\mathcal{Q}=\mathrm{column}(u,d)$, and $\hat{Q}$ is the quark electromagnetic charge operator. The normalization condition given in Eq. (25) is in a form appropriate for a single flavor configuration $\overline{q}_a q_b$, not for a multiflavor configuration state such as the ρ^0. For such states, Eq. (25) can be generalized by promoting the quark propagators to flavor matrices $\mathcal{S}=\mathrm{diag}(S^u,S^d)$, multiplying BS amplitudes Γ_μ by the appropriate flavor matrix, and tracing over flavor indices as well. The isospin-symmetric limit with $S^u=S^d$ produces BS amplitudes that are independent of flavor labels; the ρ^0 BS amplitude, for example, can then be expressed as $(\tau_3/\sqrt{2})\Gamma_\mu$ where Γ_μ is the normalized BS amplitude for the $\rho^\pm$. Use of Eq. (29) in Eq. (30) then gives

$$\frac{m_\rho^2}{g_\rho}=\frac{Z_2 N_c}{3\sqrt{2}}\int^\Lambda\frac{d^4q}{(2\pi)^4}\mathrm{Tr}_D[\gamma_\mu S^{u=d}(q+\eta P) \times\Gamma_\mu^{ab}(q;P)S^{u=d}(q-\overline{\eta}P)]=\frac{f_\rho m_\rho}{\sqrt{2}}. \tag{31}$$

The decay width $\Gamma_{\rho^0\to e^+e^-}=6.77$ keV [27] leads via

$$\Gamma_{\rho^0\to e^+e^-}=\frac{4\pi\alpha^2 m_\rho}{3g_\rho^2} \tag{32}$$

to the value $g_\rho=5.03$, that is $f_\rho=216$ MeV. Note that the isoscalar version of these considerations produces an extra factor of 1/3 on the right of Eq. (31) for the coupling of the ω to a photon. The partial width $\Gamma_{\omega\to e^+e^-}$ is indeed about 10 times smaller than $\Gamma_{\rho^0\to e^+e^-}$.

In a similar way, the coupling of the photon to the ϕ, assumed to be a pure $s\overline{s}$ state, is defined as

$$\frac{m_\phi^2}{g_\phi}\epsilon_\mu^{(\lambda)}(P)=\tfrac{1}{3}\langle 0|\overline{s}\gamma_\mu s|\phi(P,\lambda)\rangle, \tag{33}$$

and the relation between g_ϕ and the vector decay constant f_ϕ is

$$\frac{m_\phi^2}{g_\phi} = \frac{f_\phi m_\phi}{3} \tag{34}$$

$$= \frac{Z_2 N_c}{9} \int^\Lambda \frac{d^4q}{(2\pi)^4} \mathrm{Tr}_D[\gamma_\mu S^s(q+\eta P)\Gamma_\mu^{ss} S^s(q-\overline{\eta} P)]. \tag{35}$$

The partial width of the $\phi \to e^+e^-$ decay is

$$\Gamma_{\phi\to e^+e^-} = \frac{4\pi\alpha^2 m_\phi}{3 g_\phi^2}, \tag{36}$$

and the experimental value 1.37 ± 0.05 keV [27] produces $f_\phi = 237$ MeV, that is $g_\phi = 12.9$.

The decay constant f_V determines not only the coupling of the neutral vector mesons to a photon, but also the coupling of $\rho^\pm$ and $K^{\star\pm}$ to the weak vector bosons $W^\pm$. There are no data available for the leptonic decay of these charged vector mesons, but the couplings can be extracted indirectly from the decays $\tau \to \rho \nu_\tau$ and $\tau \to K^\star \nu_\tau$. The partial width for such a decay is

$$\Gamma_{\tau\to V\nu_\tau} = \frac{G_F^2 m_\tau}{8\pi} V_{ab}^2 f_V^2 m_V^2 \left(1 - \frac{m_V^2}{m_\tau^2}\right)^2 \left(1 + \frac{m_\tau^2}{2m_V^2}\right). \tag{37}$$

With the experimental values for the partial decay widths [27] $\Gamma_{\tau\to\rho\nu_\tau} = 25.02\% \Gamma_{\text{total}}$ and $\Gamma_{\tau\to K^\star\nu_\tau} = 1.28\% \Gamma_{\text{total}}$, along with the CKM matrix elements $V_{ud} = 0.974$ and $V_{us} = 0.220$, this gives a ratio

$$\frac{f_{K^\star}}{f_\rho} = 1.042 \tag{38}$$

and thus a decay constant $f_{K^\star} = 225$ MeV, if we use the experimental value $f_\rho = 216$ MeV.

With the available data, the absolute value of f_ρ using Eq. (37) gives $f_\rho = 208$ MeV. We expect, however, that the direct determination of f_ρ through $\rho^0 \to e^+e^-$, giving $f_\rho = 216$ MeV, is a more accurate determination of this decay constant. In particular, most higher-order corrections to the electroweak vertex are likely to cancel in the ratio of the partial decay widths, and therefore we use the ratio in Eq. (38) to extract the experimental $f_{K^\star}$.

V. NUMERICAL RESULTS

In Fig. 1 we show our *Ansatz* for the effective interaction, Eq. (10), for the three different parameter sets we have explored, characterized by the values of ω, together with the one-loop perturbative coupling for comparison. We use three different values of the parameter ω, constrained only by the requirement that the perturbative coupling above $q^2 = 3$ GeV^2 should be reproduced. It is only in the infrared region, below $q^2 = 2$ GeV^2, that there is a significant difference between the three parametrizations and the perturbative result. The parameter D and the current quark mass $m_{u/d}(\mu)$ are fixed by fitting m_π and f_π. Next, the strange quark mass $m_s(\mu)$ is determined by a fit to the kaon mass. The resulting value of the kaon decay constant f_K is within 3% of the experimental value, almost independent of the parameter set for the effective interaction. All three parameter sets lead to a good description of the pion and kaon masses and decay constants, as well as a reasonable value of the chiral condensate. In Table I we have summarized these results for the three different parameter sets, together with the results from Ref. [10].

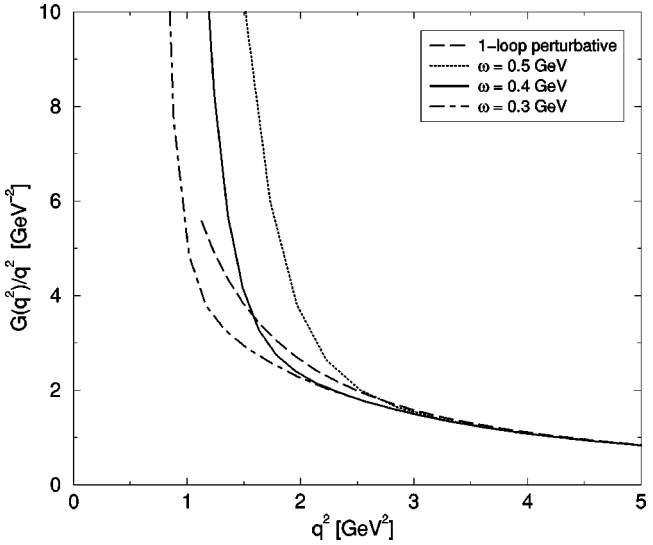

FIG. 1. The *Ansatz* for the effective $\overline{q}q$ interaction $\mathcal{G}(q^2)/q^2$, Eq. (10), for the three parameter sets, together with the one-loop perturbative result for comparison.

With our parametrization, the quark mass function $M(p^2) = B(p^2)/A(p^2)$ has qualitatively the same behavior as obtained in Ref. [10]. With a Euclidean constituent-quark mass M^E defined as the solution of $p^2 = M^2(p^2)$, we obtain constituent quark masses of about $M_{u/d} = 300 - 500$ MeV for the light quarks, and $M_s = 500 - 640$ MeV for a strange quark, spanned by the three parameter sets; the parametrization of Ref. [10] gives constituent masses $M_{u/d} = 560$ MeV and $M_s = 700$ MeV.

A. Results for vector meson observables

In Table II we present our results for the vector meson masses and decay constants. The full angular dependence was retained in the calculation of these results: we solve the set of integral equations (23) with the $F_i(p^2, p\cdot P; P^2)$ treated as functions of two variables p^2 and $z = \cos\theta$. This eigenvalue problem defines physical solutions at the mass-shell $P^2 = -m_V^2$. All calculations with the gluon *Ansatz* of Eq. (10) were performed at the physical mass shell; the calculations we have performed with the parametrization of Ref. [10] for comparison involved some extrapolation[2] to the

[2]The extrapolations were necessary because of nonanalytic behavior of the resulting quark propagator as discussed in Sec. II B.

TABLE I. Calculated values of the properties of light, pseudoscalar mesons, for the parametrization of the effective interaction (10), using three different parameter sets, and also for the parametrization of Ref. [10].

	Experiment (estimates)	Ref. [10]	$\omega=0.3$ GeV $D=1.25$ GeV^2	$\omega=0.4$ GeV $D=0.93$ GeV^2	$\omega=0.5$ GeV $D=0.79$ GeV^2
$-\langle\bar{q}q\rangle^0_{\mu=1\ \mathrm{GeV}}$	$(0.236\ \mathrm{GeV})^3$	$(0.241\ \mathrm{GeV})^3$	0.242	0.241	0.243
$m^{u=d}_{\mu=1\ \mathrm{GeV}}$	5–10 MeV	5.5 MeV	5.54	5.54	5.35
$m^{s}_{\mu=1\ \mathrm{GeV}}$	100–300 MeV	130 MeV	124	125	123
m_π	0.1385 GeV	0.1385	0.139	0.138	0.138
f_π	0.1307 GeV	0.1307	0.130	0.131	0.131
m_K	0.496 GeV	0.497	0.496	0.497	0.497
f_K	0.160 GeV	0.154	0.154	0.155	0.157

mass shell, which makes these results less accurate. In particular the integral for the normalization condition, Eq. (25), is very sensitive to such an extrapolation, which is why we do not report the decay constant for this particular model.

All parametrizations we used give equally good results for the masses and decay constants: the results are fairly insensitive to changes in ω and D, as long as they are fit to m_π, f_π, and m_K. Our result for m_ρ is typically 5% too low, whereas $m_{K^\star}$ and m_ϕ are typically 5% too large. Our result for the decay constants are within 10% of the experimental value for f_ρ and $f_{K^\star}$, and within 10 to 15 % for f_ϕ, depending on the parameter set. This agreement with experiment is quite encouraging, given the fact that the parameters are fixed by pseudoscalar observables.

The broad qualitative features of the results for the masses and decay constants shown in Table II can be obtained by using only the infrared-dominant term of our gluon *Ansatz*, that is the first term of Eq. (10). For example, the masses and decay constants for π and ρ would then be typically 5–20 % lower. However, such a model would be missing the UV behavior characteristic of QCD and this is important for some observables, such as the asymptotic form of form factors [10], that are not so dominated by the integrated infrared behavior. Furthermore, the link to QCD via the UV behavior and the associated renormalization group properties can assist greatly in future efforts to connect phenomenological models such as the present one to studies of the gluon sector of QCD via Dyson-Schwinger equations [18,19].

From Table II we can also conclude that only five of the eight covariants are qualitatively and quantitatively important for the vector meson masses and decay constants; this seems to be general, i.e., independent of the parameter set used. Of course, the relative importance of different covariants in a BS amplitude does depend on the observable under consideration. Also, use of a basis set of eight independent covariants that is different from the present basis given in Eqs. (12)–(19), could produce a different conclusion concerning the number of important covariants.

In Fig. 2 we show the behavior of the leading Chebyshev projection of the invariant amplitudes of the ρ BS amplitude ${}^0F^\rho_i(q^2;P^2)$. This and the other plots of the BS amplitudes are produced with the parameter set $\omega=0.4$ GeV and $D=0.93$ GeV^2; the results for the other parameter sets look qualitatively the same. The leading amplitudes for the pion E_π and for the rho F_1 are very similar; however, this similarity might be accidental. Of the subdominant amplitudes, F_4 and F_5 are significantly larger than the rest. The magni-

TABLE II. Comparison of the results for the vector mesons for the three different parameter sets for the effective interaction, using all eight BS amplitudes (top), and using the five leading BS amplitudes only (bottom).

	ρ		$K^\star$		ϕ	
	m_ρ	f_ρ	m_{K^*}	f_{K^*}	m_ϕ	f_ϕ
Experiment	0.770	0.216	0.892	0.225	1.020	0.237
All amplitudes F_1-F_8						
$\omega=0.3$ GeV, $D=1.20$ GeV^2	0.747	0.197	0.956	0.246	1.088	0.255
$\omega=0.4$ GeV, $D=0.93$ GeV^2	0.742	0.207	0.936	0.241	1.072	0.259
$\omega=0.5$ GeV, $D=0.79$ GeV^2	0.74	0.215	0.94	0.25	1.08	0.266
Amplitudes $F_1 \ldots F_5$ only						
Maris–Roberts Ref. [10]	0.71		0.95		1.1	
$\omega=0.3$ GeV, $D=1.20$ GeV^2	0.737	0.192	0.942	0.235	1.080	0.247
$\omega=0.4$ GeV, $D=0.93$ GeV^2	0.729	0.199	0.919	0.229	1.062	0.250
$\omega=0.5$ GeV, $D=0.79$ GeV^2	0.731	0.207	0.926	0.237	1.072	0.259

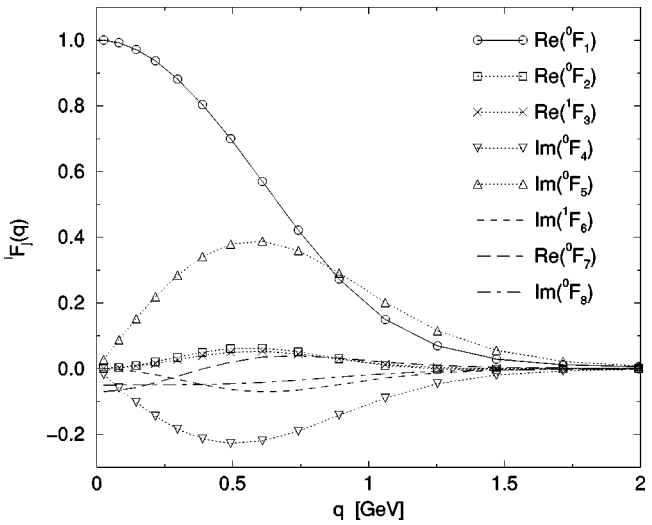

FIG. 2. The leading Chebyshev projections of all eight ρ BS amplitudes, normalized to ${}^0F_1(0)=1$, with an effective $\bar{q}q$ interaction, Eq. (10), with $\omega=0.4$ GeV, $D=0.93$ GeV^2. The most important amplitudes, F_1-F_5, are labeled by lines with symbols.

tude of the amplitudes F_6, F_7, and F_8 is much smaller than that of F_1, F_4, and F_5, as is evident from Fig. 2; this makes it understandable why these amplitudes contribute so little to the vector meson masses and decay constants. From this figure one might conclude that the amplitudes F_2 and F_3 have a similar minor role. However, it turns out that these amplitudes are essential for the convergence of the loop integral for the decay constant, Eq. (28), as discussed below, in Sec. V B.

To study the relevance of the various covariants for physical observables in more detail, we calculate the vector meson masses and decay constants using different subsets of the eight covariants in our basis. These results are given in Table III for one particular parameter set, together with the results from use of only the leading Chebyshev moments of each amplitude $F_i(q^2,q\cdot P;P^2)$. Note that the leading Chebyshev order for the $K^\star$ is zeroth order for all amplitudes F_i, in contrast to the case for the ρ and ϕ: the functions F_3 and F_6 are odd in $q\cdot P$ for the ρ and ϕ because of charge conjugation symmetry, so the leading Chebyshev order is $U_1(\cos\theta)$ for those mesons. It is evident that for the ρ and ϕ only the leading Chebyshev moment is needed to get accurate results for the masses and decay constants; but the second Chebyshev moment of F_1 is needed for strict convergence of Eq. (28). We expect this to be a general phenomenon: practical calculations of hadron observables might be facilitated by a suitable parametrization of the leading Chebyshev moments of the amplitudes F_1 through F_5. For the $K^\star$, which is not a charge conjugation eigenstate, one needs at least the zeroth and the first Chebyshev moments for an accurate description.

Another difference between the $K^\star$ and the ρ and ϕ mesons, is the dependence on the momentum sharing parameter η in Eq. (23). Charge conjugation dictates use of $\eta=0.5$ for the ρ and the ϕ. For the $K^\star$ there is no such constraint and we explored momentum partition sets $(\eta_u,\bar{\eta_s})$ varying between (0.5,0.5) and (0.4,0.6). Physical observables are in principle independent of this partitioning; any dependence of $K^\star$ physical observables on $(\eta_u,\bar{\eta_s})$ would signal an inadequacy of the ladder truncation or subsequent approximations. We find that the results for $m_{K^\star}$ and $f_{K^\star}$ are indeed unchanged under variation of the momentum sharing, as long as all covariants and the full angular dependence are taken into account. Once certain amplitudes are dropped and/or the angular dependence of the amplitudes is truncated, physical observables do become dependent on $(\eta_u,\bar{\eta_s})$: variations between (0.5,0.5) and (0.4,0.6) lead to changes in $m_{K^\star}$ and $f_{K^\star}$ of up to 5%.

TABLE III. The influence of the different covariants and of the angular dependence of the amplitudes on the vector meson properties with parameter set $\omega=0.4$ GeV, $D=0.93$ GeV^2. For this table, we have calculated the loop for the decay constant up to the renormalization point $\mu=19$ GeV, since for some of the approximations considered this integral is ultraviolet divergent. In the case of a convergent integral, the error made by cutting off the integral at the renormalization point is less than 1%.

Full angular calculation	ρ		$K^\star$		ϕ	
	m_ρ	f_ρ	$m_{K^\star}$	$f_{K^\star}$	m_ϕ	f_ϕ
All 8 amplitudes	0.742	0.207	0.936	0.241	1.072	0.259
F_1 only	0.88	0.20	>1.2		1.24	0.20
F_1, F_2, and F_3	0.90	0.17	>1.2		1.25	0.20
F_1, F_4, and F_5	0.722	0.23	0.911	0.26	1.059	0.28
$F_1\cdots F_5$	0.729	0.199	0.919	0.23	1.062	0.250
Leading Chebyshev decomposition						
All 8 amplitudes	0.743	0.211	0.92	0.24	1.074	0.262
F_1 only	0.875	0.20	1.09	0.22	1.24	0.22
F_1, F_2, and F_3	0.900	0.17	1.10		1.25	0.20
F_1, F_4, and F_5	0.724	0.23	0.90	0.26	1.062	0.28
$F_1\cdots F_5$	0.730	0.201	0.91	0.23	1.065	0.251

A comparison of the BS amplitudes of the three different vector mesons is made in Fig. 3. This figure clearly shows the difference between the ρ and ϕ mesons on the one hand, and the $K^\star$ on the other: while the leading Chebyshev moments of the ρ and ϕ amplitudes are very similar to each other and to the corresponding moments of the $K^\star$ amplitude, the latter has both even and odd moments, due to the lack of C parity. This is especially evident for the amplitudes $F_3(q,q\cdot P;P^2)$ and $F_6(q,q\cdot P;P^2)$, which have no zeroth Chebyshev moment in the case of the ρ and ϕ, but have a significant zeroth Chebyshev moment for the $K^\star$.

B. Asymptotic behavior of the BS amplitudes

The asymptotic behavior of the BS amplitudes for the ρ-meson is shown in Fig. 4, and as in the pseudoscalar case, all amplitudes behave as $1/q^2$ or $1/q^3$, up to calculable logarithmic corrections. We emphasize that in QCD these logarithmic corrections are essential for the convergence of the integral for the decay constant. Evaluation of the trace in Eq. (28) for equivalent flavors and equal momentum partitioning gives the leading behavior

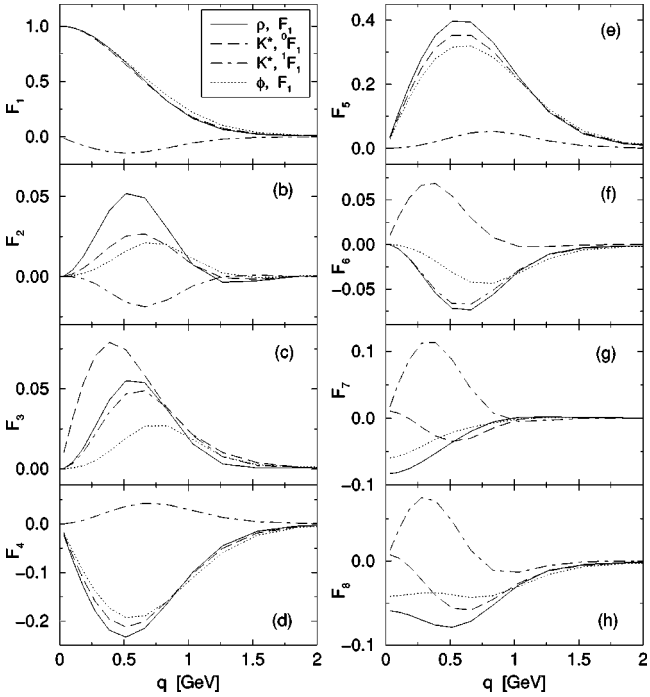

FIG. 3. Leading and subleading BS amplitudes for the ρ, $K^\star$, and ϕ mesons, (a) zeroth Chebyshev projections of F_1, and for the $K^\star$ also the first Chebyshev projection; (b) as (a), but then for F_2; (c) first Chebyshev projections of F_3, and for the $K^\star$ also the zeroth projection; (d) as (a), but then for F_4; (e) as (a), but then for F_5; (f) as (c), but then for F_6; (g) as (a), but then for F_7; (h) as (a), but then for F_8. The parameters are the same as in the previous plot: $\omega = 0.4$ GeV, $D = 0.93$ GeV^2.

$$
\begin{aligned}
f_V m_V = \frac{Z_2 N_c}{3} \int^{\Lambda} \frac{d^4q}{(2\pi)^4} \{ & [12\sigma_s^+\sigma_s^- + (4q^2 + 8q^2\cos^2\theta \\
& - 3P^2)\sigma_v^+\sigma_v^-] F_1(q^2, q\cdot P; P^2) \\
& - 32q^2(1-\cos^2\theta)^2 \sigma_v^+\sigma_v^- F_2(\cdots)/\sqrt{5} \\
& - 16q^2\cos\theta(1-\cos^2\theta)\sigma_v^+\sigma_v^- F_3(\cdots) \\
& + i8\sqrt{2}Pq(1-\cos^2\theta)\sigma_v^+\sigma_v^- F_4(\cdots) \\
& - i8q(1-\cos^2\theta)(\sigma_v^+\sigma_s^- + \sigma_s^+\sigma_v^-) F_5(\cdots) \\
& + \mathcal{O}[(F_6+F_7+F_8) q \sigma_v^{\pm}\sigma_s^{\mp}] \},
\end{aligned}
\tag{39}
$$

where $\sigma_{v,s}$ are the vector and scalar components of the quark propagator

$$
\sigma_v = \frac{A(q)}{A^2(q)q^2 + B^2(q)}, \tag{40}
$$

$$
\sigma_s = \frac{B(q)}{A^2(q)q^2 + B^2(q)}, \tag{41}
$$

and $f^{\pm} := f(q_{\pm})$. The last terms in Eq. (39), proportional to F_6, F_7, and F_8, give small and convergent contributions, since they behave in the ultraviolet as

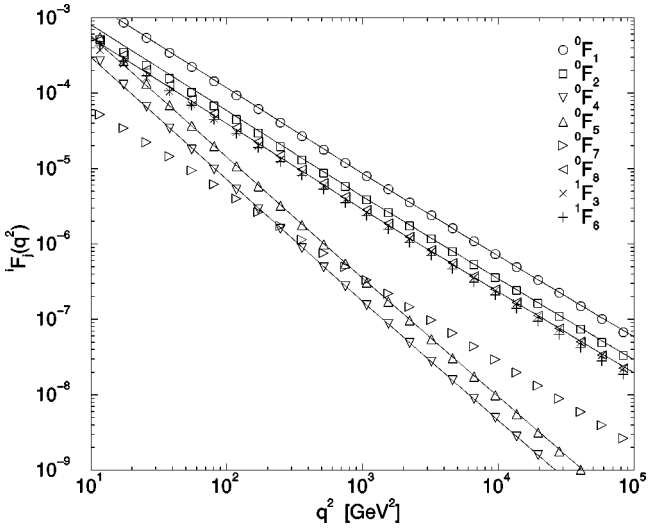

FIG. 4. The ultraviolet behavior of the ρ BS amplitudes: the leading Chebyshev moments of F_1-F_8, obtained using the full angular dependence, are shown by the symbols. The lines display the analytically calculated behavior for F_1-F_5, given by Eqs. (45)–(47), (53), and (54).

$$
F_i(q^2, q\cdot P; P^2) q \sigma_v^{\pm}\sigma_s^{\mp} \sim \frac{1}{q^5}, \tag{42}
$$

up to logarithmic corrections. Both contributions involving F_4 and F_5, which fall off as $1/q^3$, are also ultraviolet finite. Since the amplitudes F_1, F_2, and F_3 fall off as $1/q^2$, simple power counting shows that their individual contributions to Eq. (39) are logarithmically divergent, even accounting for the cutoff dependence of $Z_2(\Lambda^2, \mu^2)$.[3]

In order to analyze the asymptotic behavior produced by the vector meson BSE in more detail, we follow the strategy used in Ref. [28] for the asymptotic behavior of the function $B(p^2)$ from the quark DSE. The key step is to replace the effective running coupling $\mathcal{G}[(p-q)^2]$ by $\mathcal{G}[\max(p^2, q^2)]$. In the ultraviolet region the running coupling behaves as $1/\ln(y)$ with $y = k^2/\Lambda_{\rm QCD}^2$ which is a slowly varying function; therefore the error made in using this approximation is under control. In the infrared region, such an approximation is not to be trusted. After this approximation, and with use of the Chebyshev decomposition for the angular dependence of $F_i(q^2, q\cdot P, P^2)$ in Eq. (23), all angular integrations can be performed analytically. For the leading Chebyshev moments of the ρ BS amplitudes, Eq. (23) produces integral equations of the form

$$
\begin{aligned}
F_i(x) = & \frac{\gamma_m}{\ln x} \int_0^x dy \mathrm{K}^{ij}_{x>y}(x,y) F_j(y) \\
& + \gamma_m \int_x^{\infty} dy \mathrm{K}^{ij}_{y>x}(x,y) \frac{F_j(y)}{\ln y},
\end{aligned}
\tag{43}
$$

[3]The factor $Z_2(\Lambda^2, \mu^2)$ ensures gauge invariance and cancels logarithmic divergences in covariant gauges other than Landau gauge.

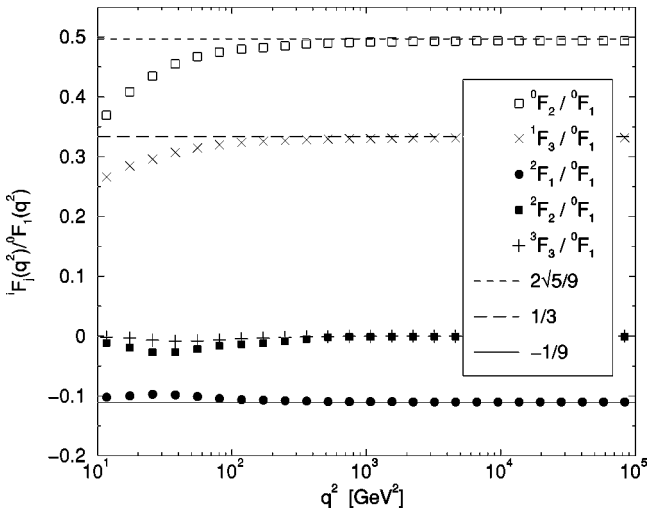

FIG. 5. The ultraviolet behavior of the ρ BS amplitudes: the ratio ${}^kF_i(q^2;P^2)/{}^0F_1(q^2;P^2)$ for the leading amplitudes.

where $x=p^2/\Lambda_{\rm QCD}^2$, $y=q^2/\Lambda_{\rm QCD}^2$, $F_i(x)={}^0F_i(q^2;P^2)$ for $i=1,2,4,5,7,8$ and $F_i(x)={}^1F_i(q^2;P^2)$ for $i=3,6$. Now the coupled integral equations can be converted to a set of coupled linear differential equations, which can be solved in the ultraviolet region by assuming a series expansion in both x and $\ln x$. For completeness, we have given the relevant kernels K^{ij} and other details in the Appendix.

The analysis in the Appendix shows that the ultraviolet behavior of the amplitudes $F_1(x)$, $F_2(x)$, and $F_3(x)$ is of the form

$$F_i(x)=\frac{a_i(\ln x)^\alpha}{x}\left(1+\sum_{j=1}^{\infty} c_j(\ln x)^{-j}\right), \tag{44}$$

and the steps leading to identification of the power α and the leading coefficients a_i are also given there. The leading ultraviolet behavior is found to be

$${}^0F_1(q^2;P^2)=F_1(x)\sim\frac{a_1(\ln x)^\alpha}{x}, \tag{45}$$

$${}^0F_2(q^2;P^2)=F_2(x)\sim\frac{a_1 2\sqrt{5}(\ln x)^\alpha}{9x}, \tag{46}$$

$${}^1F_3(q^2;P^2)=F_3(x)\sim\frac{a_1(\ln x)^\alpha}{3x}, \tag{47}$$

with

$$\alpha=-1+\gamma_m/108. \tag{48}$$

The overall constant a_1 is not determined by the homogeneous BSE; its value follows from the normalization condition.

Our numerical results show that the leading ultraviolet behavior of the BS amplitudes is governed not only by the leading Chebyshev moments ${}^0F_1(q^2;P^2)$, ${}^0F_2(q^2;P^2)$, and ${}^1F_3(q^2;P^2)$, but also by the second Chebyshev moment ${}^2F_1(q^2;P^2)$, see Fig. 5. Numerically, we find in the ultraviolet

$$\frac{{}^0F_2(q^2;P^2)}{{}^0F_1(q^2;P^2)}=0.48\pm0.01, \tag{49}$$

$$\frac{{}^1F_3(q^2;P^2)}{{}^0F_1(q^2;P^2)}=0.33\pm0.01, \tag{50}$$

$$\frac{{}^2F_1(q^2;P^2)}{{}^0F_1(q^2;P^2)}=-0.11\pm0.005, \tag{51}$$

while all other ${}^kF_i$ fall off faster. This is in excellent agreement with the analytical results for the relative magnitudes of the leading Chebyshev components, Eqs. (45)–(47). The power α of the logarithm is much harder to determine numerically; our results indicate $-0.95<\alpha<-1.0$, which is consistent with $\alpha=-0.996$ from Eq. (48). We have not studied whether the inclusion of ${}^2F_1$ in the analysis of the asymptotic behavior would change our analytical result for α; our numerical results indicate that it will not influence the coefficients a_i of ${}^0F_1$, ${}^0F_2$, and ${}^1F_3$, nor will it change the power β in Eq. (A7).

The ultraviolet behavior of the integral for the decay constant, Eq. (39), can now be analyzed in more detail. The ultraviolet behavior of the functions F_1, F_2, and F_3 does indeed lead to individual divergent integrals for $\alpha\geqslant-1$. However, the *combined* contribution is

$$f_V m_V\sim\int^{\Lambda^2} dy\,\frac{(\ln y)^\alpha}{y}\{6a_1-4\sqrt{5}a_2-4a_3+2b_1\}, \tag{52}$$

where b_1 is the coefficient of the second Chebyshev moment ${}^2F_1(q^2;P^2)$, that is, the counterpart of a_1 in Eq. (45). Use of the asymptotic behavior we have found analytically, $a_2=a_1 2\sqrt{5}/9$ and $a_3=a_1/3$, shows that the integral for the decay constant is finite if $b_1=-a_1/9$, which agrees with our numerical result, Eq. (51). This cancellation between naive divergences coming from different covariants provides an illustration of how renormalizibility is realized; it is expected since the one-loop renormalization group behavior of QCD is preserved in our rainbow-ladder truncation of the DSE and BSE. It is the vector counterpart of a similar cancellation in the integral for the pseudoscalar decay constant: numerically [10], it was found that in the ultraviolet region the π BS amplitudes satisfy $G_\pi=2F_\pi/q^2$, which makes the integral for f_π finite, although the separate contributions from F_π and G_π diverge. The above analysis, when applied to the pseudoscalar BSE, produces an asymptotic behavior of the amplitudes F_π and G_π that exactly gives $G_\pi=2F_\pi/p^2$.

Finally, in the Appendix, the same ultraviolet analysis applied to the vector BS amplitudes F_4 and F_5 gives

$$F_4(x)\sim\frac{a_4}{x^{3/2}(\ln x)^{1-(1/3)\gamma_m}}, \tag{53}$$

$$F_5(x) \sim \frac{a_5}{x^{3/2}(\ln x)^{1-(1/2)\gamma_m}}. \quad (54)$$

In principle, the influence of F_6, F_7, and F_8 might change the power of the logarithm for F_4 or F_5, but we expect no change in the leading ultraviolet behavior of F_1, F_2, and F_3.

VI. CONCLUDING REMARKS

We have calculated the light vector meson masses and the decay constants associated with electromagnetic and leptonic decays using the ladder truncation for the meson BSE in conjunction with the rainbow truncation for the quark DSE. We use an effective quark-antiquark interaction $\mathcal{G}(k^2)/k^2$ with one phenomenological parameter, which is fitted to reproduce f_π; the two other parameters are the current quark masses $m_{u/d}$ and m_s which are fixed through m_π and m_K. The calculated values for the vector meson masses are within 5% of the experimental values; the decay constants are within 10% of their experimental values. These results are fairly robust: they are weakly dependent upon the scale at which the interaction starts to deviate from the perturbative behavior, as long as the parameters are fitted to pseudoscalar observables.

An earlier BSE study [16] in a related framework produced qualitatively comparable results for m_ρ, $m_{K^\star}$, and m_ϕ as part of a study that included heavy mesons and incorporated five quark flavors. Vector meson decay constants were not considered. That approach produced a dependence upon the momentum-sharing parameter η that is stronger than what we find. The present results for physical observables, such as the mass and decay constant, are *independent* of the momentum sharing, as long as all relevant covariants and the full angular dependence are included in the calculation. A recent work [29] has explored the feasibility of extracting ground state vector meson masses from the large Euclidean time behavior of the quark current-current correlator as calculated from the ladder truncation of the inhomogeneous BSE for the vector vertex. Only the ρ was studied, the BS amplitudes were not extracted and the decay constant was not calculated.

Of the eight allowed transverse covariants, five are both quantitatively and qualitatively important, whereas the remaining three amplitudes contribute little to the mass and decay constant. Neglect of these three amplitudes changes the calculated masses by only 2% and decay constants by 8%. For the ρ and ϕ the dependence of the BS amplitudes on $q\cdot P$ is very small; truncation to the leading Chebyshev moments leads to very similar results. However, the second moment of F_1 is needed for convergence of the loop integral for the decay constant. This suggests that, in general, hadronic observables can be well described by a rather limited number of covariants and Chebyshev moments. For the $K^\star$, however, more Chebyshev moments are required, since it is not a charge conjugation eigenstate. Our numerical results can be used to guide the development of approximating forms for the BS amplitudes for calculation of a variety of observables such as electromagnetic form factors and strong decays typified by $\rho\to\pi\pi$ and $\phi\to KK$.

The ladder truncation of the BSE is known to be a good approximation for flavor nonsinglet pseudoscalar mesons [17], and it is expected to be reliable for vector mesons as well. This is to be contrasted with the scalar channel, where the same analysis revealed [30] that the next-order corrections are much more important. For flavor-singlet mesons, there are also contributions from diagrams corresponding to quark annihilation to timelike gluons. These play an important role for pseudoscalars, e.g., in the generation of the η' mass through the axial anomaly [31]. For the flavor-singlet vector mesons however, there is no such anomaly. Also, if quark annihilation diagrams play a major role for such mesons one would expect more flavor mixing than is evident for the ω and ϕ. It is therefore reasonable to expect the ladder truncation to be appropriate for vector mesons. For the ground state vector mesons considered here, there is an open decay channel to a pair of pseudoscalars (e.g., $\rho\to\pi\pi$), but this is a P-wave coupling that tends to suppress the mechanism relative to such a decay of a scalar. Estimates of the effects of meson loops on the ρ mass vary between 2 and 10 % [32]. With the BS amplitudes calculated here we expect to be able to investigate the effects of meson dressing more accurately in the future. Note that both the meson dressing and the quark annihilation diagrams can contribute to the splitting between the ρ and ω, which are degenerate in the ladder truncation.

The confinement property embedded within the dynamically dressed propagators in the present BSE approach raises the prospect of studies of excited state light-quark mesons without unphysical quark decay thresholds. However, a straightforward application of the present calculational technique is limited by the complex p^2-plane singularities that arise in the quark propagator DSE solutions in rainbow approximation. As the meson mass increases, the integration region for the mass-shell BSE solution in Euclidean metric covers a larger complex domain and such complex singularities will eventually be encountered. This may be an artifact of the ladder-rainbow truncation. A different calculational procedure that may alleviate these difficulties is to base the approach upon the relevant current-current correlator where the meson momentum remains spacelike and is Fourier transformed to a large Euclidean time [29]. The meson ground state mass is identifiable from the exponential fall-off with time. The numerical accuracy of that approach as well as the feasibility of obtaining excited state masses and isolating the associated BS amplitude are topics that require further study.

The task of modeling vector mesons within QCD at finite temperature and chemical potential has recently begun with extremely simplified Ansätze for the kernel of the BSE [33]. The present work may provide valuable guidance for the extension and improvement of such efforts to explore the behavior of vector $\bar{q}q$ states and correlations relevant to chiral restoration and quark deconfinement transitions.

ACKNOWLEDGMENTS

We acknowledge useful conversations and correspondence with C.D. Roberts, L.S. Kisslinger, and D. Jarecke.

This work was funded by the National Science Foundation under Grant No. PHY97-22429, and benefited from the resources of the National Energy Research Scientific Computing Center.

APPENDIX: ASYMPTOTIC BEHAVIOR OF THE BS AMPLITUDES

In order to analyze the asymptotic behavior of the BS amplitudes ${}^iF_j(q^2;P^2)$, we have to perform all angular integrals analytically. These angular integrals have measure

$$\int d\Omega_{p,q} := \frac{2}{\pi^2}\int_0^\pi d\theta_p \sin^2\theta_p \int_0^\pi d\theta_q \sin^2\theta_q \int_0^\pi d\phi \sin\phi = 1, \tag{A1}$$

where θ_p is the angle between the external momentum p and P, and θ_q is the angle between the integration momentum q and P. This type of integral can be performed with the help of the appendix of Ref. [34], and some typical results are

$$\int d\Omega_{p,q} \frac{p\cdot q}{(p-q)^2} = \frac{pq\ \min(p,q)}{2\ \max(p,q)^3}, \tag{A2}$$

$$\int d\Omega_{p,q} \frac{p\cdot q}{(p-q)^4} = \frac{pq\ \min(p,q)}{\max(p,q)^3[\max(p,q)^2-\min(p,q)^2]}. \tag{A3}$$

Other, more complicated, integrals can be expressed in a similar way. A common feature of these angular integrals is that they can all be expressed in terms of $\max(p,q)$ and $\min(p,q)$. This allows us to convert the integral equations to differential equations [28].

We have performed all the angular integrals in the five coupled integral equations for ${}^0F_1(q^2;P^2)$, ${}^0F_2(q^2;P^2)$, ${}^1F_3(q^2;P^2)$, ${}^0F_4(q^2;P^2)$, and ${}^0F_5(q^2;P^2)$, ignoring the functions F_6, F_7, and F_8, and truncating the Chebyshev moments at the leading order. With the leading ultraviolet behavior of the functions F_1, F_2, and F_3 considered first, the relevant kernels are

$$\mathrm{K}^{11}_{x>y}(x,y) = \frac{1}{4x}, \quad \mathrm{K}^{11}_{y>x}(x,y) = \frac{x}{4y^2},$$

$$\mathrm{K}^{12}_{x>y}(x,y) = \frac{-\sqrt{5}}{6x}, \quad \mathrm{K}^{12}_{y>x}(x,y) = \frac{-\sqrt{5}(4y-x)}{18y^2},$$

$$\mathrm{K}^{13}_{x>y}(x,y) = \frac{-1}{6x}, \quad \mathrm{K}^{13}_{y>x}(x,y) = \frac{-(4y-x)}{18y^2},$$

$$\mathrm{K}^{21}_{x>y}(x,y) = \frac{-\sqrt{5}(4y-3x)}{54x^2}, \quad \mathrm{K}^{21}_{y>x}(x,y) = \frac{-\sqrt{5}x}{54y^2},$$

$$\mathrm{K}^{22}_{x>y}(x,y) = \frac{5(9y-8x)}{216x^2}, \quad \mathrm{K}^{22}_{y>x}(x,y) = \frac{5x^2}{216y^3},$$

$$\mathrm{K}^{23}_{x>y}(x,y) = \frac{-\sqrt{5}(8x-3y)}{216x^2}, \quad \mathrm{K}^{23}_{y>x}(x,y) = \frac{-5\sqrt{5}x^2}{216y^3},$$

$$\mathrm{K}^{31}_{x>y}(x,y) = \frac{-(4y-3x)}{36x^2}, \quad \mathrm{K}^{31}_{y>x}(x,y) = \frac{-x}{36y^2},$$

$$\mathrm{K}^{32}_{x>y}(x,y) = \frac{-\sqrt{5}(8x-3y)}{144x^2}, \quad \mathrm{K}^{32}_{y>x}(x,y) = \frac{-5\sqrt{5}x^2}{144y^3},$$

$$\mathrm{K}^{33}_{x>y}(x,y) = \frac{17y-8x}{144x^2}, \quad \mathrm{K}^{33}_{y>x}(x,y) = \frac{(25x-16y)x}{144y^3}. \tag{A4}$$

These are to be inserted into the integral equation (43), which is

$$F_i(x) = \frac{\gamma_m}{\ln x}\int_0^x dy \mathrm{K}^{ij}_{x>y}(x,y)F_j(y) + \gamma_m \int_x^\infty dy \mathrm{K}^{ij}_{y>x}(x,y)\frac{F_j(y)}{\ln y}, \tag{A5}$$

where $F_i(x) = {}^0F_i(q^2;P^2)$ for $i=1,2$ and $F_3(x) = {}^1F_3(q^2;P^2)$. This set of coupled integral equations can now be converted into a set of coupled fourth-order differential equations for $F_{1-3}(x)$ of the type

$$x^4\kappa_{4i}F_i''''(x) + x^3\kappa_{3i}F_i'''(x) + x^2\kappa_{2i}F_i''(x) + x\kappa_{1i}F_i'(x) + \kappa_{0i}F_i(x) = 0. \tag{A6}$$

Substitution of the series expansion

$$F_i(x) = \frac{a_i(\ln x)^\alpha}{x^\beta}\left(1 + \sum_{j=1}^{\infty} c_i^j (\ln x)^{-j}\right) \tag{A7}$$

into the set of differential equations leads to a set of coupled equations for the powers α and β, and the leading coefficients a_i. It is easy to see that all terms in the differential equation have the same power of x, and collection of all the leading powers of $\ln x$ gives an equation for the power β. One of the solutions of this equation is $\beta=1$, which is obviously the physical solution, see Fig. 4. The next-to-leading order terms lead to three coupled equations for the four constants α, a_1, a_2, and a_3; the homogeneous BSE allows for an arbitrary overall scaling and we set $a_1=1$. The solution for the other constants is then

$$\alpha = -1 + \frac{\gamma_m}{108}, \tag{A8}$$

$$a_2 = \frac{2\sqrt{5}}{9}, \tag{A9}$$

$$a_3 = \frac{1}{3}. \tag{A10}$$

Note that the powers α and β are the same for all three functions. Differences between these functions arise only from differences in the leading coefficients a_i, and in the subleading coefficients c_i^j.

Next we consider ${}^0F_4$, which decouples from the other amplitudes after performing the angular integrals. The only nonzero kernels in Eq. (A5) are

$$\mathrm{K}^{44}_{x>y}(x,y)=\frac{\sqrt{y}}{x^{3/2}},\quad \mathrm{K}^{44}_{y>x}(x,y)=\frac{\sqrt{x}}{y^{3/2}}. \tag{A11}$$

The resulting asymptotic behavior can be expressed by Eq. (A7) with

$$\beta_4=\tfrac{3}{2}, \tag{A12}$$

$$\alpha_4=-1+\tfrac{1}{3}\gamma_m. \tag{A13}$$

This is in agreement with the numerical result, see Fig. 4. The equation for F_5 is more complicated, since ${}^0F_5$ does couple to ${}^0F_1$, ${}^0F_2$, and ${}^1F_3$. The relevant kernels are

$$\mathrm{K}^{51}_{x>y}(x,y)=\frac{M(y)}{2x^{3/2}},\quad \mathrm{K}^{51}_{y>x}(x,y)=\frac{\sqrt{x}M(y)}{2y^2},$$

$$\mathrm{K}^{52}_{x>y}(x,y)=\frac{\sqrt{5}M(y)}{3x^{3/2}},\quad \mathrm{K}^{52}_{y>x}(x,y)=\frac{\sqrt{5}\sqrt{x}M(y)}{3y^2},$$

$$\mathrm{K}^{53}_{x>y}(x,y)=\frac{M(y)}{3x^{3/2}},\quad \mathrm{K}^{53}_{y>x}(x,y)=\frac{\sqrt{x}M(y)}{3y^2},$$

$$\mathrm{K}^{55}_{x>y}(x,y)=\frac{\sqrt{y}}{2x^{3/2}},\quad \mathrm{K}^{55}_{y>x}(x,y)=\frac{\sqrt{x}}{2y^{3/2}}. \tag{A14}$$

However, a careful analysis shows that the leading ultraviolet behavior of ${}^0F_5$ is not influenced by coupling to other amplitudes; the leading behavior arises from K^{55} only. The result is Eq. (A7) with

$$\beta_5=\tfrac{3}{2}, \tag{A15}$$

$$\alpha_5=-1+\tfrac{1}{2}\gamma_m, \tag{A16}$$

also in agreement with our numerical results, see Fig. 4. The influence of ${}^0F_5$ on our previous results for ${}^0F_1$, ${}^0F_2$, and ${}^1F_3$ can be examined for consistency. Those three amplitudes fall off like $1/x$, while contributions from ${}^0F_5$ to these amplitudes via the differential equations in Eq. (A6) will be suppressed by a factor of $M(x)/\sqrt{x}$, and thus contribute to the subleading behavior only.

[1] P. Maris, C. D. Roberts, and P. C. Tandy, Phys. Lett. B **420**, 267 (1998).
[2] M. A. Ivanov, Yu. L. Kalinovsky, and C. D. Roberts, Phys. Rev. D **60**, 034018 (1999).
[3] C. D. Roberts, Nucl. Phys. **A605**, 475 (1996); C. J. Burden, C. D. Roberts, and M. J. Thomson, Phys. Lett. B **371**, 163 (1996).
[4] M. R. Frank, K. L. Mitchell, C. D. Roberts, and P. C. Tandy, Phys. Lett. B **359**, 17 (1995); D. Kekez, B. Bistrovic, and D. Klabucar, Int. J. Mod. Phys. A **14**, 161 (1999).
[5] R. Alkofer and C. D. Roberts, Phys. Lett. B **369**, 101 (1996).
[6] P. C. Tandy, Prog. Part. Nucl. Phys. **39**, 117 (1997).
[7] F. Hawes and M. A. Pichowsky, Phys. Rev. C **59**, 1743 (1999).
[8] M. A. Pichowsky and T.-S. H. Lee, Phys. Lett. B **379**, 1 (1996); Phys. Rev. D **56**, 1644 (1997).
[9] C. J. Burden, Lu Qian, C. D. Roberts, P. C. Tandy, and M. J. Thomson, Phys. Rev. C **55**, 2649 (1997).
[10] P. Maris and C. D. Roberts, Phys. Rev. C **56**, 3369 (1997).
[11] M. R. Frank and C. D. Roberts, Phys. Rev. C **53**, 390 (1996).
[12] P. C. Tandy, Fiz. B **8**, 295 (1999).
[13] C. D. Roberts and A. G. Williams, Prog. Part. Nucl. Phys. **33**, 477 (1994).
[14] N. Brown and M. R. Pennington, Phys. Rev. D **39**, 2723 (1989).
[15] See, for example, C. D. Roberts, A. G. Williams, and G. Krein, Int. J. Mod. Phys. A **4**, 1681 (1992); F. T. Hawes, C. D. Roberts, and A. G. Williams, Phys. Rev. D **49**, 4683 (1994); Sec. (6.2) of Ref. [13]; P. Maris, Phys. Rev. D **52**, 6087 (1995).
[16] P. Jain and H. J. Munczek, Phys. Rev. D **48**, 5403 (1993).
[17] A. Bender, C. D. Roberts, and L. v. Smekal, Phys. Lett. B **380**, 7 (1996).
[18] L. v. Smekal, A. Hauck, and R. Alkofer, Phys. Rev. Lett. **79**, 3591 (1997); Ann. Phys. (N.Y.) **267**, 1 (1998).
[19] D. Atkinson and J. C. R. Bloch, Phys. Rev. D **58**, 094036 (1998); Mod. Phys. Lett. A **13**, 1055 (1998).
[20] D. Leinweber, J. I. Skullerud, and A. G. Williams, Phys. Rev. D **58**, 031501 (1998).
[21] F. T. Hawes, P. Maris, and C. D. Roberts, Phys. Lett. B **440**, 353 (1998).
[22] H. J. Munczek and A. M. Nemirovsky, Phys. Rev. D **28**, 181 (1983).
[23] S. J. Stainsby and R. T. Cahill, Int. J. Mod. Phys. A **7**, 7541 (1992).
[24] P. Maris and H. Holties, Int. J. Mod. Phys. A **7**, 5369 (1992).
[25] C. J. Burden, C. D. Roberts, and A. G. Williams, Phys. Lett. B **285**, 347 (1992).
[26] J. Gasser and H. Leutwyler, Phys. Rep. **87**, 77 (1982).
[27] Particle Data Group, C. Caso *et al.*, Eur. Phys. J. C **3**, 1 (1998).
[28] D. Atkinson and P. W. Johnson, Phys. Rev. D **37**, 2296 (1988).
[29] T. Meissner and L. S. Kisslinger, Phys. Rev. C **59**, 986 (1999).
[30] C. D. Roberts, in *Quark Confinement and the Hadron Spectrum II*, edited by N. Brambilla and G. M. Prosperi (World Scientific, Singapore, 1997), pp. 224–230.
[31] J. Kogut and L. Susskind, Phys. Rev. D **10**, 3468 (1974).

[32] L. C. L. Hollenberg, C. D. Roberts, and B. H. J. McKellar, Phys. Rev. C **46**, 2057 (1992); D. B. Leinweber and T. D. Cohen, Phys. Rev. D **49**, 3512 (1994); K. L. Mitchell and P. C. Tandy, Phys. Rev. C **55**, 1477 (1997); M. A. Pichowsky, S. Walawalkar, and S. Capstick, Phys. Rev. D **60**, 054030 (1999).

[33] P. Maris, C. D. Roberts, and S. Schmidt, Phys. Rev. C **57**, 2821 (1998); D. Blaschke and P. C. Tandy, in *Understanding Deconfinement in QCD*, edited by D. Blaschke, F. Karsch, and C. D. Roberts (World Scientific, Singapore, in press).

[34] P. Maris and Q. Wang, Phys. Rev. D **53**, 4650 (1996).